

# Effect of Te addition on some physical properties of the $\text{Se}_3\text{S}_2$ system and a study of the response to $\gamma$ -irradiation

A. F. MAGED, L. A. WAHAB, I. A. EL KHOLY

National Center for Radiation Research and Technology, Atomic Energy Authority  
PO Box 29, Nasr City, Cairo, Egypt

Glasses based on sulphur and tellurium were carefully characterized to establish the interdependence between chemical composition and the magnitudes of the physical parameters related to their use as infrared optical materials. Parameters considered in this paper are density, molar volume, transition temperatures, crystallization activation energy, decomposition energy, direct current (d.c.) electrical properties, optical energy gap and infrared transmission spectra in the range  $400\text{--}6000\text{ cm}^{-1}$ . The  $\gamma$  irradiation has no detectable effect on both the d.c. conductivity of the bulk glass and the optical energy gap.

© 1998 Kluwer Academic Publishers

## 1. Introduction

Numerous chalcogenide glass-forming systems have been evaluated as sources for new infrared (IR) optical materials. Chalcogenide glasses exhibit a wide variety of photoinduced phenomena that enable them to be used as optical imaging or storage media [1] and are also well-known IR-transmitting materials [2] having wide transmission (depending on composition) from the visible to beyond  $15\ \mu\text{m}$  [3]. Some investigators have pointed out [4–6] that several other parameters are important when evaluating an IR optical material for use with high-energy  $\text{CO}_2$  lasers emitting at  $10.6\ \mu\text{m}$ . IR and Raman techniques have been used for obtaining information about the structure of chalcogenide glasses [7]. The aim of this work is to study some physical parameters and the effect of  $\gamma$ -rays on the fundamental absorption edge at room temperature and the direct-current (d.c.) electrical conductivity at low temperatures by using nitrogen for  $\text{Se}_3\text{S}_{2-x}\text{Te}_x$  systems with  $x = 0.0, 0.5, 1.0, 1.5$  and  $2.0$ .

## 2. Experimental procedures

Glass samples of the system  $\text{Se}_3\text{S}_{2-x}\text{Te}_x$  where  $x = 0.0, 0.5, 1.0, 1.5$  and  $2.0$  were prepared by the usual melt-quench technique [8]. The binary glass composition containing Se and S corresponding to  $\text{Se}_3\text{S}_2$  (purity, 99.999%) were weighed and sealed in an evacuated silica glass tube which was then inserted in an electric furnace maintained at  $200^\circ\text{C}$  for 3 h then  $350^\circ\text{C}$  for 3 h. The tube was frequently agitated in order to intermix the constituents to ensure homogeneity of the melt. The melt was then quenched in ice-water. The ternary glasses  $\text{Se}_3\text{S}_{2-x}\text{Te}_x$  were prepared by adding Te (purity, 99.99%) to the binary  $\text{Se}_3\text{S}_2$  in an evacuated silica glass tube. The tube was

then inserted in a furnace and the temperature was raised in steps, first to  $250^\circ\text{C}$  for 2 h, then to  $350^\circ\text{C}$  for 2 h and finally to  $600^\circ\text{C}$  for 2 h. The molten liquid was frequently shaken to ensure homogeneity in the melt. The melt was then quenched in ice-water. The density of the glass was determined by the hydrostatic weighing of the glass in benzene and was calculated using Myuller's [9] formula  $\rho_{\text{th}} = \sum_i (P_i/d_i)^{-1}$ , where  $P_i$  is the fraction of the weight of the  $i$ th structural unit and  $d_i$  is the corresponding density. The concept of the small polaron is well known. The excess electron so distorts the surrounding lattice that the potential well thereby generated is deep enough to induce localization. Polarons have been studied in ordered and disordered solids. For the polaron to be small, the polaron radius,  $r_p$ , must be greater than the radius of the atom on which the electron is localized, but less than the distance,  $R$ , separating these sites. The polaron radius can be determined from the relation given by [10]

$$r_p = \frac{1}{2} \left( \frac{\pi}{6N} \right)^{1/3} \quad (1)$$

where  $N$  is the number of Te atoms per unit volume which could be calculated by using the Naster-Kingery [11] formula. Hence the polarons should decrease in size as the number of atoms increases.

$$N = \frac{\rho_{\text{glass}} P N_A}{AW100} \quad (2)$$

where  $\rho_{\text{glass}}$  is the density of the glass,  $N_A$  is Avogadro's number,  $AW$  is the atomic weight of the Te (in grams), and  $P$  is the weight percentage of Te in the glass matrix. The average spacing of Te-Te in the

glass was calculated from

$$R = \left( \frac{1}{N} \right)^{1/3} \quad (3)$$

The molar volume,  $V$ , of the glass, (i.e., the volume occupied by 1 g-molecule of the glass), was calculated from the expression  $V = (xM_a + yM_b + zM_c)/\rho_g$ , where the glass composition is represented by  $x$ ,  $y$  and  $z$  ( $x + y + z = 100\%$ ),  $M_a$ ,  $M_b$  and  $M_c$ , are the molecular weights of materials a, b and c forming the glassy network and  $\rho_g$  is the experimental density. The differential scanning calorimetry analysis was carried out at a constant heating rate of  $10^\circ\text{C min}^{-1}$  using a Shimadzu series 50. The transformed fraction  $\alpha'$  was calculated using the relation  $\alpha' = A(T)/A(\text{total})$  where  $A(T)$  is the area under the peak of crystallization through certain interval of temperature and  $A(\text{total})$  is the total area under the peak of crystallization. The electrical conductivity of the bulk materials was measured at temperature between about 20 and  $-110^\circ\text{C}$ . The specimen was initially ground flat and the edges were made parallel with thickness of between 0.35 and 0.45 mm. Circular silver electrodes (sandwich type) were painted on each side of the specimen. The film samples were deposited by the thermal evaporation technique using an Edward 306E coating unit in a vacuum of  $10^{-6}$  Torr on cleaned glass slide substrates. The thickness of these films were determined with a thickness monitor. Thin films employed for d.c. conductivity measurements were primarily coated with coplanar electrodes separated by a gap of width 2 mm. A Shimadzu UV-160A spectrophotometer was used for the absorption measurements with the necessary facility to eliminate the effect of substrates. For measurements of  $\alpha$  greater than  $10^3 \text{ cm}^{-1}$ , a thin film of each material was evaporated on a glass slide and the absorption was measured. The IR absorption spectra of the studied glass samples were measured using a Fourier transform IR Unicam Mattson-1000 spectrophotometer using the KBr disc technique, over the spectral range  $400\text{--}6000 \text{ cm}^{-1}$ . All IR measurements were carried out at room temperature. Glass samples of 1 mg were thoroughly mixed and ground with 200 mg of KBr, after which the mixture were pressed at 10 tons (disc diameter, 1.3 cm) for 10 min under vacuum to yield transparent discs suitable for mounting in the spectrometer and determining the absorption spectra [12]. The X-ray diffraction pattern of the produced bulk and thin film on glass slide showed no clear sharp lines, confirming the amorphous nature of the samples except for  $x = 2$ .

### 3. Results and discussion

The values of the glass density,  $\rho_g$ , the molar volume,  $V$ , the calculated concentration of Te atoms in the glass, the small-polaron radius,  $r_p$ , the average space,  $R$ , of Te atoms in the glass, the glass transition temperature,  $T_g$ , the temperature,  $T_c$ , of crystallization and the melting temperatures,  $T_m$ , of all glasses are shown in Tables I and II. For ternary glasses both  $\rho_g$  and  $V$  depended on the Te concentration. The change in

TABLE I Glass compositions, densities, molar volumes, the concentrations of Te atoms per unit volume, the average spacings of Te atoms and the small-polaron radii deduced from the density

Composition	$\rho$ ( $\text{g cm}^{-3}$ )	$V$ ( $\text{cm}^3$ )	$N \times 10^{22}$ ( $\text{cm}^{-3}$ )	$R$ ( $\text{\AA}$ )	$r_p$ ( $\text{\AA}$ )
$\text{Se}_3\text{S}_2$	3.86	15.61	—	—	—
$\text{Se}_3\text{S}_{1.5}\text{Te}_{0.5}$	4.04	17.25	1.91	4.43	1.79
$\text{Se}_3\text{S}_1\text{Te}_1$	4.55	17.43	2.0	4.37	1.77
$\text{Se}_3\text{S}_{0.5}\text{Te}_{1.5}$	5.05	17.61	2.38	4.13	1.67
$\text{Se}_3\text{Te}_2$	5.47	18.00	2.58	4.02	1.62

TABLE II Transition temperature as a function of composition at a heating rate of  $10^\circ\text{C min}^{-1}$  where  $T_x$  is the united crystallization temperature and  $T_p$  is the Maximum crystallization temperature

Composition	$T_g$ ( $^\circ\text{C}$ )	$T_c$ ( $^\circ\text{C}$ ) $T_x$	$T_p$	$T_m$ ( $^\circ\text{C}$ )	$k_g$	$E_a$ (eV)	$E_d$ eV
$\text{Se}_3\text{S}_2$	55	95	99	134	0.56	4.27	2.51
$\text{Se}_3\text{S}_{1.5}\text{Te}_{0.5}$	60	115	125	209	0.44	3.96	2.25
$\text{Se}_3\text{S}_1\text{Te}_1$	65	91	110	275	0.21	3.20	1.87
$\text{Se}_3\text{S}_{0.5}\text{Te}_{1.5}$	66	92	99	285	0.15	3.11	1.0
$\text{Se}_3\text{Te}_2$	67	81	109	286	0.19	2.65	0.88

$V$  was due to the change in structure caused by the variation in interatomic spacing, which could be attributed to the change in the number of bonds per unit volume of the glassy network. The value of  $\rho_g$  increases from 3.86 to 4.04, 4.55, 5.05 and  $5.47 \text{ gm cm}^{-3}$ , respectively, as shown in Table I. So, the molar volume of the ternary glass system would be higher than the binary  $\text{Se}_3\text{S}_2$  glass, as shown in Table I. From the change in molar volume it was clear that the corresponding structural unit, with its surrounding space, increases by introducing tellurium metal into the glass network, i.e., the basic structural units are linked more randomly. The number of Te atoms per unit volume, the average spacing of Te atoms and the small-polaron radius are obtained from density measurements and are shown in Table I. For low concentrations of Te the energy levels associated with the presence of Te would be likely to form a band as the minimum Te concentration (i.e., for  $\text{As}_{576}\text{S}_{863}\text{Te}_1$ ) would be high enough for significant interaction between the appropriate electrons; the average spacing of the Te atoms in  $\text{As}_{576}\text{S}_{863}\text{Te}_1$  is about  $33.4 \text{ \AA}$  and that of the Te atoms in the other alloy glasses is less [13]. Table II shows the transition temperatures, the glass transition,  $T_g$ , the crystallization temperature,  $T_c$ , and the melting temperature,  $T_m$ . The exothermic transformation takes place between 99 and  $125^\circ\text{C}$  for  $x = 0$  and 0.5, respectively. The activation energies,  $E_a$ , of  $\text{Se}_3\text{S}_{2-x}\text{Te}_x$  glass systems were calculated by the Avrami [14] method as shown in Table II. The value of  $T_g$  increases with increasing tellurium concentration. This may indicate a tendency for stronger bonding in tellurium-rich glasses. Also from Table II it can be seen that the crystallization peak ( $T_c$ ) increases with increasing Te to S ratio at a constant heating rate. The glass-forming tendency,  $k_{gl}$ , which was a useful parameter in comparing the devitrification tendency of the

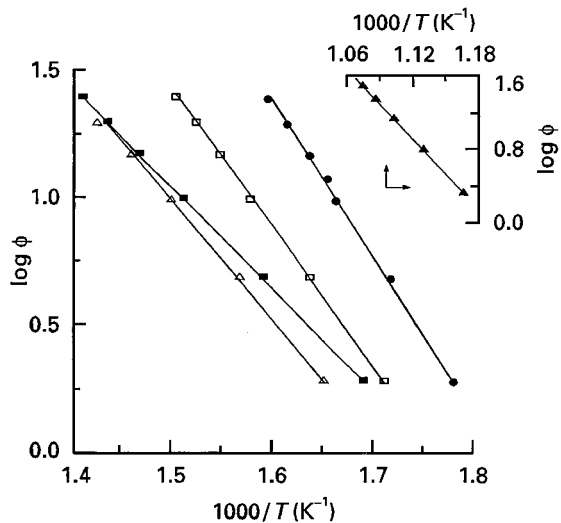


Figure 1 Relation between  $\log \phi$  and  $1000/T$  as obtained from thermogravimetric analysis of the  $\text{Se}_3\text{S}_{2-x}\text{Te}_x$  glass system. (●),  $\text{Se}_3\text{S}_2\text{Te}_0$ ; (□),  $\text{Se}_3\text{S}_{1.5}\text{Te}_{0.5}$ ; (■),  $\text{Se}_3\text{S}_1\text{Te}_1$ ; (△),  $\text{Se}_3\text{S}_2\text{Te}_{1.5}$ ; (▲),  $\text{Se}_3\text{S}_0\text{Te}_2$ .

glass is given by  $k_{gl} = (T_c - T_g)/(T_m - T_g)$  [15]. The variation in  $\log \phi$  (from thermal gravimetry thermograms) versus  $1/T$ , where  $\phi$  is the heating rate for all system (2, 5, 10, 15, 20 and  $25^\circ\text{C min}^{-1}$ ) is shown in Fig. 1. The activation energy,  $E_d$ , of decomposition is useful for evaluating the thermal stability of materials, and the  $E_d$  values were calculated by the Ozawa [16] method. Table II shows a decrease in  $E_d$  with increase in Te concentration.

The measurements of electrical conductivity as a function of temperature as shown in Fig. 2. The values obtained for the electrical energy gap,  $E_\sigma$ , from the conductivity and the values of the conductivity,  $\sigma_{RT}$ , at room temperature (about  $20^\circ\text{C}$ ) are shown in Table III. Values of  $E_\sigma$  and  $\sigma_{RT}$  are plotted in Fig. 3 in the same manner as that used by Farag and Edmond [13]; also plotted (Fig. 3, line A) is a line represented by the equation  $\sigma = \sigma_0 \exp(-E_\sigma/2kT)$ . If the mobilities of the carriers were constant and not activated, this line would represent the variation in the carrier concentration in the glasses. One cannot normally deduce much about the mechanism of conductivity from measurements only of conductivity versus temperature. Nevertheless, it should be possible to see whether the measurements could be consistent with

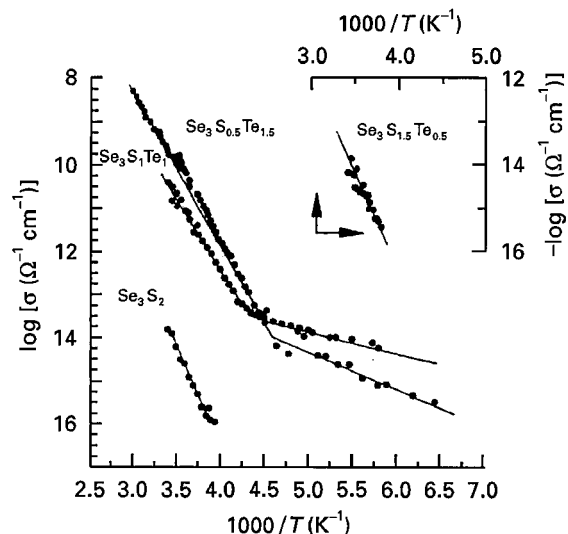


Figure 2 Temperature dependence of the d.c. conductivity of the  $\text{Se}_3\text{S}_{2-x}\text{Te}_x$  glass system.

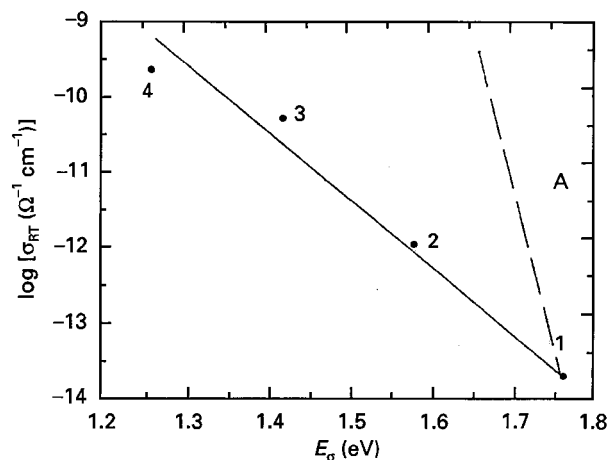


Figure 3 Conductivity of the glass system versus  $E_\sigma$  for  $\text{Se}_3\text{S}_2$  (point 1),  $\text{Se}_3\text{S}_{1.5}\text{Te}_{0.5}$  (point 2),  $\text{Se}_3\text{S}_1\text{Te}_1$  (point 3) and  $\text{Se}_3\text{S}_{0.5}\text{Te}_{1.5}$  (point 4). Line A is drawn through point (1) for  $\text{Se}_3\text{S}_2$  with a slope given by the equation  $\sigma = \sigma_0 \exp(-E_\sigma/2kT)$ .

the results of optical absorption and our suggested explanation.

The values of the optical gap,  $E_{opt}$ , of these films with various tellurium concentrations is shown in Table III. Band theory for crystalline semiconductors suggests that the absorption coefficient,  $\alpha$ , in an

TABLE III Values of the measured parameters of bulk and thin film compositions associated with optical absorption and electrical conduction; in the last column,  $\theta_{opt}^D$  corresponds to the optical Debye temperature;  $\delta E = E_\sigma(\text{Se}_3\text{S}_2) - E_\sigma(\text{ternary})$

Composition	Bulk $\sigma_{RT} \times 10^{-14}$ ( $\Omega^{-1} \text{cm}^{-1}$ )	Thin film		$E_\sigma$ (eV)	$\delta E$ (eV)	$E_{opt}$ (eV)	$E_\sigma - E_{opt}$ (eV)	$\Delta E$ (eV)	$\beta^{-1} \times 10^{-6}$ (cm eV)	$\theta_{opt}^D$ (K)
		$E_\sigma$ (eV)								
		First	Second							
$\text{Se}_3\text{S}_2$	1.54	1.76	—	1.79	0.0	1.58	0.21	0.52	1.085	575
$\text{Se}_3\text{S}_{1.5}\text{Te}_{0.5}$	90.3	1.58	—	1.70	0.09	1.31	0.49	0.57	1.230	575
$\text{Se}_3\text{S}_1\text{Te}_1$	4770	1.42	0.22	1.18	0.61	1.15	0.03	0.60	1.070	575
$\text{Se}_3\text{S}_{0.5}\text{Te}_{1.5}$	22600	1.26	0.27	1.14	0.65	1.04	0.10	0.64	1.030	575
$\text{Se}_3\text{Te}_2$	—	—	—	0.69	1.1	1.02	-0.33	0.66	0.746	575

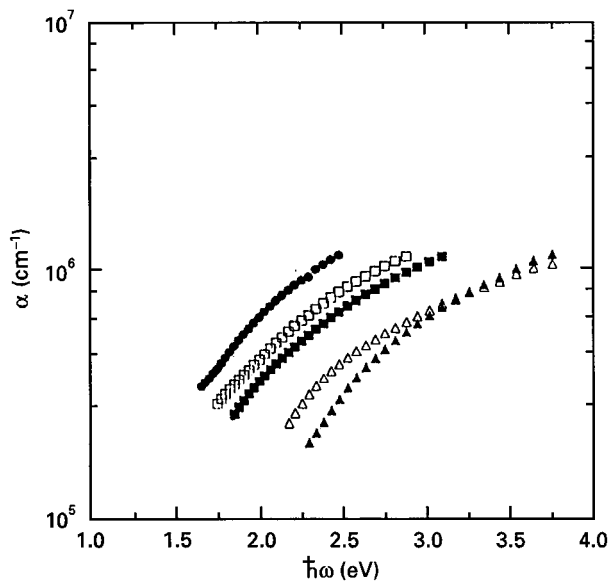


Figure 4 Absorption coefficient as a function of photon energy for the  $\text{Se}_3\text{S}_{2-x}\text{Te}_x$  glass system. ( $\blacktriangle$ ),  $\text{Se}_3\text{S}_2$ ; ( $\triangle$ ),  $\text{Se}_3\text{S}_{1.5}\text{Te}_{0.5}$ ; ( $\blacksquare$ ),  $\text{Se}_3\text{S}_1\text{Te}_1$ ; ( $\square$ ),  $\text{Se}_3\text{S}_{0.5}\text{Te}_{1.5}$ ; ( $\bullet$ ),  $\text{Se}_3\text{Te}_2$ .

indirect transition can be written as  $\alpha = \text{constant} \cdot |M|^2 (\hbar\omega - E_{\text{opt}})^2 / \hbar\omega$ , where  $M$  is the matrix element of the electrical transition. If  $M$  is constant, plotting  $(\alpha\hbar\omega)$  against  $\hbar\omega$  should result in a straight line [17]. The optical gap is obtained by intersection of this line with the energy axis. Quite a high concentration of Te produces a large displacement of the absorption edge as shown in Fig. 4 towards the lower energy. Consider Fig. 5, which shows a simple structure network with increasing concentration of Te, i.e., atoms  $\text{Te}'$  and  $\text{Te}''$ , etc., successively replacing S atoms. It seems probable

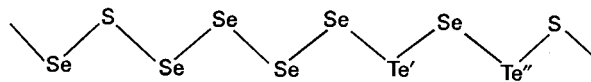


Figure 5 A structure (without disorder) for  $\text{Se}_3\text{S}_{2-x}\text{Te}_x$ . The ratio of the numbers of atoms would correspond to  $\text{Se}_6\text{S}_2\text{Te}_2$  or  $\text{Se}_3\text{S}_1\text{Te}_1$ .

that the addition of the first atom,  $\text{Te}'$ , could produce a new electron level relatively deep into the pseudogap, while the addition of the second atom,  $\text{Te}''$ , while adding to the number of levels, would only have a small effect on the position of the levels. We note that Table I that the Te atoms are not far apart (their separation is down to about 4.4 Å on average in  $\text{Se}_3\text{S}_1\text{Te}_1$ ) and their separation may vary owing to compositional and network disorders. Hence the Te atoms could interact and produce subbands (as distinct from localized states suggested by Kosek et al. [18]) and we would expect the push-out to be large at first, but then to increase more slowly with increase in  $x$ .

The IR transmittance as a function of wavenumber is shown in Fig. 6. The peaks at 1600, 2300 and 3400  $\text{cm}^{-1}$  presumably are due to dissolved gases. They are variable in magnitude and in intensity relative to one another. The presence of these bands reflects the evolution of some gases from diffusion oil during evacuation, perhaps the presence of residual dissolved gases in the reactants and probably the evolution of  $\text{H}_2\text{O}$  from silica during the seal-off process. The Debye temperature  $\theta_{\text{opt}}^{\text{D}}$  was taken to be the temperature characteristic of the lower peak in the vibration spectrum ( $\hbar\omega_0/K$ ) [19]. The  $\gamma$  irradiation has no detectable effect on both the d.c. conductivity of bulk glass (up to 28 Mrad) and the optical energy gap of the

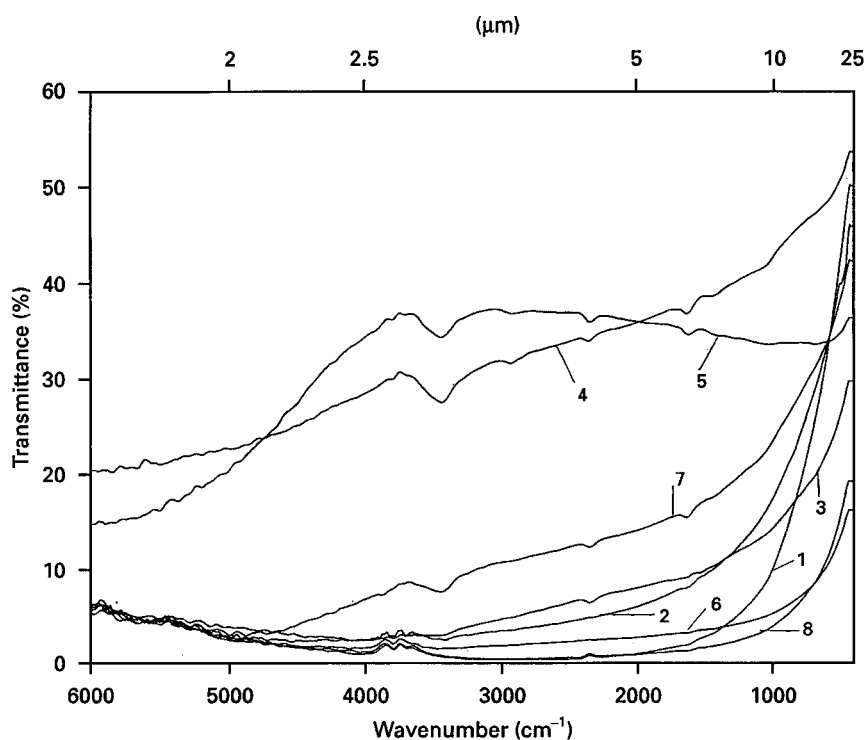


Figure 6 IR transmission spectra for the  $\text{Se}_3\text{S}_{2-x}\text{Te}_x$  glass system, (glass powder, 1 mg; KBr, 100 mg). Curve 1, pure Te; curve 2, pure S, curve 3, pure Se; curve 4,  $\text{Se}_3\text{S}_2$  glass (amorphous); curve 5,  $\text{Se}_3\text{S}_{1.5}\text{Te}_{0.5}$  (amorphous); curve 6,  $\text{Se}_3\text{S}_1\text{Te}_1$  (amorphous); curve 7,  $\text{Se}_3\text{S}_{0.5}\text{Te}_{1.5}$  (amorphous); curve 8,  $\text{Se}_3\text{Te}_2$  (crystalline).

thin film (upto 8 Mrad). Our result are consistent with the optical gap of system  $(\text{As}_2\text{Se}_3)_{1-x}\text{Te}_x$  [20] and contradict the effect of  $\gamma$  radiation on both the optical energy gap of oxide glass [21] and a thermoluminescence study in amorphous semiconductors  $\text{Si}_x\text{Te}_{60-x}\text{As}_{30}\text{Ge}_{10}$  system [22].

#### 4. Conclusion

On the basis of the physical parameter data presented here, on changing completely from a sulphur base to a tellurium base and considering only the physical properties, an increase was observed in the density (about 42%), the molar volume (about 15%), the glass transition temperature (about 22%) and the maximum crystallization temperature (about 10%). A decrease was observed in the d.c. electrical energy gap of bulk (about 28%) and the optical energy gap of the thin film (about 35%). The  $\gamma$  irradiation has no detectable effect on the electrical and optical properties. This system with  $x = 0.5$  is considered to be a good IR-transmitting material in the night vision range (8–12  $\mu\text{m}$ ).

#### References

1. A. E. OWEN, A. P. FIRTH and P. J. S. EWEN, *Phil. Mag. B* **52** (1985) 347.
2. J. A. SAVAGE and K. L. LEWIS, *Proc. SPIE* **683** (1986) 79.
3. A. ZAKERY, A. ZEKAK, P. J. S. EWEN, C. W. SLINGER and A. E. OWEN, *J. Non-Cryst. Solids* **114** (1989) 109.

4. M. SPORKS, *J. Appl. Phys.* **42** (1971) 5029.
5. A. R. HELTON, *J. Electron. Mater.* **2** (1973) 211.
6. B. BENDOW, *ibid.* **3** (1974) 201.
7. T. OHSAKA, *J. Non-Cryst. Solids* **17** (1975) 121.
8. S. A. FAYEK, M. H. EL FOULY, H. H. AMER and M. M. EL OCKER, *J. Solid State Commun.* (1995) 213.
9. R. L. MYULLER, "Khimia, Tverdovo Tela" (*Leningrad Univeristy, Leningrad, 1965*) Chapter 9.
10. V. BOGOMOLOV, E. KUDINOV and Y. FRISOV, *Sov. Phys.-Solid State* **9** (1967) 3175.
11. H. H. NASTER and W. D. KINGERY, in Proceedings of the Seventh International Conference on Glass, Brussels, 1965 (Gordon and Breach, New York, 1965) p. 106.
12. A. ABDEL-KADER, R. EL-MALLAWANY and M. M. EL. KHOLY, *J. Appl. Phys.* **73** (1993) 71.
13. A. FARAG and J. T. EDMOND, *Phil. Mag. B* **53** (1986) 413.
14. M. J. AVRAMI, *Chem. Phys.* **9** (1941) 177.
15. F. BRANDA, A. MAROTTA and A. BURI, *Thermochim. Acta* **144** (1989) 117.
16. T. OZAWA, *Polymers* **13** (1971) 150.
17. J. TAUC, A. ABRAHAM, R. ZALLEN and M. SLADE, *J. Non-cryst. Solids* (1970) 279.
18. F. KOSEK, A. CIMPL, R. HLADINA, J. TULKA and J. KOCKA, *ibid.* **37** (1980) 31.
19. M. SAYER and A. MANSINGH, *Phys. Rev. B* **6** (1972) 4629.
20. S. A. FAYEK and A. F. MAGED, *Mater. Sci. Engng* **B32** (1995) 47.
21. A. F. MAGED and F. ABDEL REHIM, *Appl. Radiat. Isot. J. Radiat. Appl. Instrum. A* **42** (1991) 763.
22. A. F. MAGED, Y. M. AMIN and S. A. DURRANI, *J. Mater. Sci.* **27** (1992) 5536.

Received 9 April 1997

and accepted 2 April 1998